UNIVERSITY OF OSLO

THE DECAY OF HOT DYSPROSIUM NUCLEI

A. Atac, J. Rekstad, M. Guttormsen,
S. Messelt and T. Ramsøy

Department of Physics, University of Oslo,
Oslo, Norway

and

T.F. Thorsteinsen, G. Løvhøiden and T. Rødland
Department of Physics, University of Bergen,
Norway

OUP--

Report 87-10

Received 19/03 - 1987

ISSN-0332-5571

DEPARTMENT OF PHYSICS

REPORT SERIES

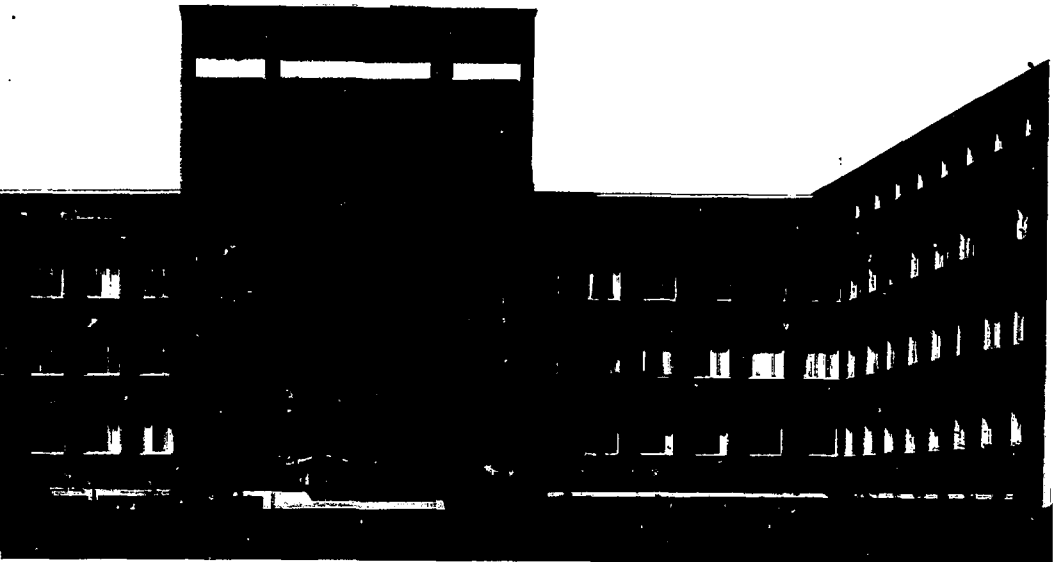

THE DECAY OF HOT DYSPROSIUM NUCLEI

A. Atac, J. Rekstad, M. Guttormsen,
S. Messelt and T. Ramsøy

Department of Physics, University of Oslo,
Oslo, Norway

and

T.F. Thorsteinsen, G. Løvhøiden and T. Rødland
Department of Physics, University of Bergen,
Norway

Report 87-10 Received 19/03 - 1987

ISSN-0332-5571

THE DECAY OF HOT DYSPROSIUM NUCLEI

A. Ataç, J. Rekstad, M. Guttormsen, S. Messelt and T. Ramsøy

Institute of Physics, University of Oslo, Oslo, Norway

and

T.F. Thorsteinsen, G. Løvhøiden and T. Rødland

Institute of Physics, University of Bergen, Bergen, Norway

Abstract:

The γ-decay following the ^{162,163}Dy(^{3}He,αxn) reactions with $E_{^3He}$ = 45 MeV has been studied. Non-statistical γ-radiation with energies of $E_\gamma \approx 1$ MeV and ≈ 2 MeV is found for various residual nuclei. The properties of these γ-ray bumps depend on the number of emitted neutrons and reveal an odd-even mass dependence. New techniques to extract average neutron energies as a function of excitation energy and of the number of emitted neutrons are employed. The deduced neutron energies are consistent with Fermi-gas model predictions.

NUCLEAR REACTION ^{162,163}Dy(^{3}He,αxn), $E_{^3He}$ = 45 MeV; measured $\sigma(E_\alpha)$, E_γ, I_γ,$\alpha\gamma$-coincidence. Deduced γ-ray multiplicity, neutron energy. Enriched targets, Ge, NaI, Si detectors. Fermi-gas model analysis.

1 Introduction

In this paper we investigate the decay properties of some Dy nuclei in an excitation energy region from the ground state up to the threshold for fission. The nuclei are excited through the (^{3}He,α) one particle transfer reaction. The nuclear spin is therefore restricted by the range of single particle angular momenta available. In the (^{3}He,α) process we expect the excitation energy to be distributed over various intrinsic modes of motion, which makes it possible to associate the excitation of the nucleus with a heating process.

In general thermodynamics, temperature is a concept defined for states of equilibrium. Such a condition may not be fulfilled for nuclear states. A sufficient density of states, and a lifetime long enough to ensure that the energy supplied is distributed statistically on the various degrees of freedom in the system, are both necessary conditions. In the discussion below we compare the experimental results with expectations from such a thermodynamical picture of the nucleus. Both the emission of particles in evaporation-like spectra and the shape of the statistical γ-ray spectra give support to the relevance of the concept.

The aim of this investigation is to gain further insight into the structure of states built up by intrinsic excitations and about the physical laws that govern this interplay of nucleonic motion. The method employed is to study the detailed peak structures as well as the gross properties in the spectra of γ-rays emitted from the various excitation energy regions.

2 Experimental method and results

Selfsupporting targets of ^{162}Dy and ^{163}Dy, isotopically enriched to 96% and 97% respectively, were bo. rded with 45 MeV ^{3}He particles from the MC 35 cyclotron at the University of Oslo. Charged particles and γ-rays were detected in a set-up consisting of four $\Delta E - E$ particle telescopes and four γ-ray detectors. The technique employed is described in detail in a previous paper [1].

The particle telescopes were placed symmetrically around the beam axis at 40° forward angle. The ΔE and E Si detectors had thicknesses of 150 μm and 3000 μm and were used to select α-particles with energies between 20 MeV and 60 MeV. The Q-values for the ^{162}Dy(^{3}He,α)^{161}Dy and ^{163}Dy(^{3}He,α)^{162}Dy reactions are 12.6 MeV and 14.4 MeV, respectively. Thus we were able to study the region from the ground state up to approximately 40 MeV of excitation energy under the present experimental conditions. The total solid angle for the four telescopes was 0.26 sr, and the average energy resolution (FWHM) was around 300 keV.

The experimental singles α-particle yield recorded as a function of energy is shown in fig.1 for the two reactions. The analysis of the (^{3}He,α) spectra were hampered by the impurities of carbon and oxygen in the targets giving rise to significant α-particle peaks, as clearly seen in the upper part of fig.1.

Separate experiments were carried out with a foil of natural carbon and a thin paper as targets. From these spectra a contamination spectrum was constructed with the same ratio between carbon and oxygen as in the dysprosium experiments. In the lower part of fig.1 are shown the spectra from the two reactions after subtraction of the contamination spectrum. All impurity peaks were not removed from the spectra in this way. Among these, the broad peak at around 44 MeV is presumably the result of a pile-up peak from the ΔE counters. This contribution is particularly unpleasant in the spectrum from the ^{162}Dy(^{3}He,α) reaction.

A comparison of the two corrected spectra shows that the α-particle yield varies less than 30% for α-particle energies between 20 and 53 MeV. Consequently, for a scattering angle of 40°, the (^{3}He,α) reaction excites the Dy nuclei with approximately constant probability for excitation energies ranging from a few MeV up to nearly 40 MeV.

Singles α-particle spectra were recorded along with the particle-γ coincident events. Two 19% Ge detectors provided high resolution γ-ray spectra which are employed to identify various residual nuclei by their yrast transitions. Two 5" × 5" NaI counters, equipped with appropriate lead-collimators, recorded the γ-radiation with a total detection efficiency approximately independent of the γ-ray energy. The NaI spectra were used to determine the average γ-ray energy and the γ-multiplicity as a function of excitation energy.

Alpha-coincident γ-ray spectra recorded with the Ge detectors are shown in fig.2. The upper spectrum is from the ^{162}Dy(^{3}He,αxn) reaction and the lower one from the ^{163}Dy(^{3}He,αxn) reaction, with no restrictions on the α-particle energy. Consequently, the spectra represent the total yield from the reactions and provide information about the relative channel cross sections. The even-even final nuclei are easily identified from the limited number of prominent ground band transitions, in contrast to the odd nuclei where the decay is spread over several competing transitions.

In the γ-ray spectrum from the ^{163}Dy(^{3}He,αxn) reaction the yrast transitions from three even-even final products are easily identified. The relative intensity ratios of the $4^+ - 2^+$ transitions in ^{162}Dy, ^{160}Dy and ^{158}Dy are 1.0 : 1.2 : 0.3, respectively, in this case relatively low population of ^{158}Dy is due to the energy threshold of the particle detectors. In the radiation following the ^{162}Dy(^{3}He,αxn) reaction the intensity ratio is 1.0 : 1.1 for ^{160}Dy and ^{158}Dy.

Since the intensities of γ-rays from the even-even products are approximately equal, these nuclei account for equal fractions of the total reaction yield. Furthermore, since the differential (^{3}He,α) cross-section at $\theta = 40°$ is nearly constant in the studied energy region, these yields are led from equally wide excitation energy domains of the α-particle spectra.

3 Gamma-decay properties

3.1 Feeding regions

Figure 3 shows α-particle spectra obtained with gates on prominent γ-lines in the Ge spectra (see fig.2) which are known to belong to the decay of the various Dy isotopes. These α-particle groups show the energy regions in the nucleus directly created in the transfer process which feed the various final isotopes. These feeding regions are the results of the balance between the two decay modes; particle evaporation and γ-decay.

The ground band transitions contain a major part of the total yield, therefore the corresponding feeding regions are well established. However, the total γ-decay intensity in the odd nuclei is widely spread on many transitions giving less significance in the results for these nuclei. As seen from fig.3, the extracted α-particle yield for ^{161}Dy is particularly weak.

It is evident from the lower part of fig.3 that the heaviest products in both reactions have fairly well separated feeding regions. This fact illustrates that neutron evaporation is much more favourable than γ-decay in cases where both processes are energetically possible. When more than one neutron evaporate , the associated α-particle spectrum becomes more like a Gaussian distribution, indicating the competition between the neighbouring channels. At higher n channels, the α-particle distributions tend to have extentions towards lower α-particle energies. This feature is clearly visible in the feeding regions of ^{160}Dy from both reactions. Here, the data indicate that neutrons with energies as high as 10-12 MeV are emitted.

Table 1 shows the centroids and FWHM values deduced from the feeding regions in fig.3. The FWHM values are rather constant for the n = 1-3 channels. This confirms the conclusion of sect.2 that various regions constitute nearly identical effective widths. Relatively low FWHM values of the 0n channels, feeding regions of ^{161}Dy and ^{162}Dy, are due to their well-separated particle groups. The low FWHM value of the 4n channel is a result of the energy threshold of the particle detectors.

3.2 Decay strengths

The γ-ray decay pattern of various final Dy nuclei can be studied in detail by gating on the appropriate feeding regions shown in fig.3. The most pronounced γ-lines in the gated Ge spectra of the even-even nuclei belong to the yrast transitions, which is also seen in fig.2. However, in the gated Ge spectra transitions between vibrational states and the ground band members are also evident.

The γ-decay strengths for various isotopes are shown in fig.4. The uncertainties of the intensities of resolved lines are estimated to be 10% , rising to 50% for the weakest ones. The total side-feeding into the yrast band is determined from the

intensities of the yrast transitions. The intensities noted as *unresolved* represent the side-feeding not accounted for by the discrete lines.

Figure 4 demonstrates that the relative importance of the various decay routes changes with the number of emitted neutrons. The ^{163}Dy(^{3}He,α)^{162}Dy channel reveals decay of high lying ($E_x > 2$ MeV) levels with one branch feeding directly into the ground band and another branch going into the vibrational bands. Both routes seem to have the same strength. However, for the $2n$ channel (^{160}Dy) a direct feeding into the ground band seems more favoured than the decay via the vibrational bands. In ^{158}Dy, where 4 neutrons are evaporated, mainly the direct feeding to the ground band levels is observed. The same trend is seen in the ^{162}Dy(^{3}He,αxn) reaction for the residual ^{160}Dy and ^{158}Dy nuclei. The γ-strength which feeds directly into the ground band increases with a factor of 1.6 as the number of emitted neutrons increases from 0 to 4. The spin distribution of the side feeding to the yrast states does not show any systematic changes, although there is a tendency that the width increases with the number of emitted neutrons. Thus, the change in decay routes cannot be explained by differences in the populated spins only.

The observed differences in the decay routes may be related to changes in the average structure of the populated daughter nuclei, due to the evaporation of neutrons. The emission of neutrons will presumably smear out or remove particular structures of the nuclear states, e.g. single- or two-quasiparticle configurations of dominance.

3.3 Gamma-ray bumps

Further information about the γ-decay properties is obtained from the coincident γ-ray NaI spectra of fig.5. Apart from the low energy yrast transitions, the intenities of the γ-ray spectra decrease exponentially as a function of γ-ray energies for both even-even and odd-even nuclei (indicated by the dashed lines in fig.5). However, the spectra of nuclei produced in the few n channels show deviations from this statistical shape.

The heaviest even-even reaction products exhibit two γ-ray bumps which are superimposed on the statistical shape. One of them is centered around a γ-ray energy of 1 MeV and the other one, which is wider, is located slightly above 2 MeV. A general decrease in the strength of the bump structures is observed as the number of emitted neutrons increases. For ^{158}Dy the bump structure is completely washed out. The γ-ray spectra of the odd mass nuclei reveal a 2 MeV bump with roughly the same strength as for the even-even nuclei. However, the 1 MeV bump is absent.

The bump structures have been observed earlier in several deformed rare earth nuclei[2,3,4]. We therefore believe that these bumps represent a characteristic γ-decay pattern of highly excited low spin states in deformed nuclei. Their significant contribution to the total γ-decay make them of considerable interest.

In order to gain insight into these nonstatistical structures, simulations[5] of the γ-decay within a Fermi-gas have been performed. The γ-decay from a certain energy region E_x is estimated using the Monte Carlo technique with the decay probability function

$$P(E_\gamma) \propto E_\gamma^n \, \rho(E_x - E_\gamma) \, . \qquad (1)$$

Here, E_γ is the γ-ray energy and ρ is the level density which is computed in the excitation energy region after the γ-emission. The exponent n is believed to be between 3 and 5 [6]. In the lowest excitation energy region ($E_x < 2$ MeV), the level density can be approximated by counting the levels. For higher excitation energies ($E_x > 2$ MeV), a level density function of the independent Fermi-gas model with pairing is used (see Richter[7]).

The simulations indicate that the 1 MeV and 2 MeV bumps originate from the lowest excitation energy region where a large variation in the level density is present. Qualitatively, the 1 MeV bump corresponds to transitions from the lowest lying two quasiparticle states ($E_x \approx 2$ MeV) to the vibrational states ($E_x \approx 1$ MeV) and from the vibrational states to the ground band states. The model gives contribution to the 2 MeV bump from transitions originating from two quasiparticle states ($E_x \approx 2$ MeV) decaying into the ground band. By this interpretation, the bump structures represent the two groups of transitions shown in fig.4.

An explanation of the 2 MeV bump in the odd system is given by Chen and Leander using the particle-rotor model[8,9]. They explain the occurence of the bump by the favoured interband M1 γ-ray transitions between the widely separated high-j orbitals.

4 Gamma-ray multiplicity

The γ-ray multiplicities of the ^{162}Dy(^{3}He,α) and ^{163}Dy(^{3}He,α) reactions are shown in fig.6. These spectra are obtained by dividing the α-particle spectra taken in coincidence with γ-rays measured in the NaI counters by the corresponding singles α-particle spectra. A γ-ray energy threshold of 430 keV was chosen for the NaI counters in order to obtain an almost constant detection probability as a function of E_γ. Since the ground band transitions have energies below this threshold, the γ-ray multiplicity spectra of fig.6 include statistical or quasistatistical γ-cascades, only. The absolute normalization of the multiplicity spectra is determined with an accuracy of 20% .

For α-particle energies above the neutron binding energy B_n, the multiplicity increases with decreasing α-particle energy in both nuclei. There is a sudden drop in multiplicity just below B_n. This sharp edge in the multiplicity spectrum demonstrates that neutron emission dominates as soon as this decay mode is energetically possible. The γ-ray multiplicity below B_n is due to the γ-ray transitions in the daughter nucleus after the neutron emission. Also, the evaporation of two neutrons at α-particle energies just below B_{2n} is associated with a decrease in multiplicity for both reactions. The multiplicity curve reveals a possible even-odd

mass dependence. In the even-even nuclei the multiplicity reaches a maximum of about 4 and approximately one unit less in the odd nuclei due to the lower neutron threshold there.

Similar sudden drops are not clearly observed in the lower α-particle energy region. This may be due to the competition between the neighbouring channels. In the high excitation energy region (low α-particle energy) the multiplicity has values close to the maximum for the even-even nuclei, even though the γ-ray emitters in this region are both of even-even and odd-A type.

The increase in multiplicity with excitation energy is probably associated with the change in the decay routes as shown in fig.4. The decay routes which populate directly the ground band seem to contribute with a higher multiplicity than the decay routes which also include the population of vibrational states localized in the 1.0 - 1.5 MeV excitation energy region.

5 Determination of neutron energies

The experimental data provide information about gross properties of the neutrons emitted after the transfer reaction even though the neutrons are not directly observed. Thus, the features of these neutrons are deduced from the observed α-particle and γ-ray quantities. An outline of the technique is given below.

Let us assume that the pick-up process leaves the nucleus with an excitation energy E_x, sufficient for a forthcoming evaporation of x neutrons. Thus, the energy relation

$$E_x = \sum_{i=1}^{x} \epsilon_i + B_{xn} + E'_x \tag{2}$$

is fulfilled, where B_{xn} is the threshold energy for the emission of x-neutrons, E'_x is the excitation energy of the daughter nucleus before γ-decay and ϵ_i is the energy carried by a neutron. It follows that

$$< \bar{\epsilon} >= 1/x(< E_x > - B_{xn} - < E'_x >) \, , \tag{3}$$

where

$$\bar{\epsilon} = 1/x \sum_{i=1}^{x} \epsilon_i \, . \tag{4}$$

The excitation energy $< E'_x >$ is connected to the γ-ray multiplicity by

$$< E'_x >=< E_\gamma >< M_\gamma > \, . \tag{5}$$

An analysis of the average neutron energy as a function of excitation energy can be carried out using eq.(3). The γ-ray multiplicity of ^{162}Dy as a function

of excitation energy is shown in fig.7. Above the neutron binding energy, the multiplicity curve corresponds to transitions in ^{161}Dy. This spectrum is compared to a fit to the multiplicity curve obtained in the ^{162}Dy(^{3}He,α) reaction (dashed curve). The difference between the two slopes is related to the energy carried away by the emitted neutron. The average neutron energy $< \epsilon >$ obtained in this way (it corresponds to the x=1 case of eq.(3)) is shown as a function of the excitation energy in fig.8. It should be noted that the experimental conditions correspond to an average over all neutron angles. Unfortunately, the impurity which lies around E_x = 44 MeV (see sect.2) prevents a detailed investigation. However, an increase in the average neutron energy is evident by increasing excitation energy. A linear fit to the data (solid line) gives a rate of $d\epsilon/dE_x$ = (0.3 $\pm$ 0.1) and an average neutron energy of $< \bar{\epsilon} >$ = (1.3 $\pm$ 0.3) MeV. These values are averaged beetween excitation energies of 1 MeV and 8 MeV above the neutron threshold of E_x B_n.

In a statistical description of the compound nucleus, the average neutron energy is related to the temperature of the final nucleus[10] as $< \epsilon > \sim 2T$. Thus, the increasing average neutron energy in fig.8 indicates an increasing temperature in the daughter nucleus by the excitation energy. The average temperature for the 1n channel deduced from the above given neutron energy is (0.65 $\pm$ 0.15) MeV.

The experimental data permits us to employ a different method to study the average neutron energies also at the higher xn channels. Here, we apply eq.(3), where $< E_x >$ is determined as the center of gravity for the α-particle groups of fig.3 which are taken in coincidence with γ-rays in the corresponding daughter nucleus. The average excitation energy $< E'_x >$ can be evaluated from the γ-ray multiplicity $< M_\gamma >$, by using eq.(5) where the average γ-ray energy $< E_\gamma >$ is determined from the NaI γ-ray spectra.

The resulting average neutron energies $< \bar{\epsilon} >$, are shown in fig.9 as a function of the number of emitted neutrons. The average neutron energy in the 1n channel of the ^{163}Dy(^{3}He,α) reaction is calculated to be (1.4 $\pm$ 0.2) MeV in perfect agreement with the data of fig.8. When 2 and 3 neutrons are evaporated the average energy increases to approximately 2 MeV.

A theoretical estimate (dashed line in fig.9) is obtained with the computer code Cascade which calculates the neutron evaporation spectra after the formation of a compound nucleus in statistical equilibrium. Further details on this model are given in ref.[11]. The employed angular momentum distributions and excitation energy regions were determined from the experimental yrast population and the position of the particle groups of fig.3. Level densities were calculated from the Fermi-gas model and the level density parameter is adjusted to give the best fit to the experimental results. The model reproduces the data satisfactorily. The sudden increase in neutron energy from 1n to 2n is described quite well. However, the odd-even staggering effect is not accounted for in the present model.

6 Summary

The decay properties of several Dy nuclei were studied using the ^{162}Dy(^{3}He,αxn)$^{161-s}$Dy and ^{163}Dy(^{3}He,αxn)$^{162-s}$Dy reactions up to an excitation energy of about 40 MeV above the ground states of ^{161}Dy and ^{162}Dy.

The γ-transitions observed in the Ge spectra of the even-even Dy nuclei could be classified into two groups : (i) yrast transitions, (ii) transitions from vibrational band states into the ground band and (iii) transitions feeding directly into the ground band. It was found that the relative number of transitions via the vibrational states to transitions feeding the ground band states directly change significantly with the number of emitted neutrons.

This dependence is also reflected in the NaI γ-ray spectra. The heaviest even-even nuclei produced directly or by one neutron emission exhibit two γ-ray bumps superimposed on a statistical spectrum, with γ-ray energies of 1 MeV and 2 MeV. The odd-even products feature a 2 MeV bump, only. Fermi-gas model calculations indicate that thes bumps originate from the lowest excitation energy region where the low lying continuum states feed into the ground band either directly or via vibrational states. The bumps lose their strength in the spectra of the lighter reaction products. The change in decay pattern can be related to a temperature or spin effect which is not completely understood. However, supported by the consistent occurence of these structures in several nuclei, we conclude that they are characteristics in the γ-decay of highly excited low spin states.

The γ-ray multiplicity spectrum exhibits the decay properties of states above and below the neutron threshold. The sudden drop in the multiplicity curve around the neutron binding energy demonstrates that neutron emission dominates as soon as it is energetically possible. Bumps associated with one and two neutron emissions are visible in the multiplicity spectra. Due to the competition between neighbouring neutron channels, three and four neutron emissions are not well separated by the multiplicity.

The experimental data allow us to extract neutron energies as a function of the excitation energy in the ^{163}Dy(^{3}He,αn)^{161}Dy reaction. Here, the average nuclear temperature is (0.65 $\pm$ 0.15) MeV. Furthermore, we have obtained estimates on the average neutron energy as a function of the number of emitted neutrons. Apart from a possible odd-even mass dependence, the results are consistent with statistical model calculations.

References:

1. J. Rekstad, A. Henriquez, F. Ingebretsen, G. Midttun, B. Skaali, R. Øyan, J. Wikne, T. Engeland, T.F. Thorsteinsen, E. Hammarén and E. Liukkonen, Phys. Scr. **T5**(1983)45

2. A. Henriquez, J. Rekstad, F. Ingebretsen, M. Guttormsen, K. Eldhuset, B. Nordmoen, T. Ramsøy, R. Renstrøm-Pedersen, R.M. Aasen, T.F. Thorsteinsen and E. Hammarén, Phys. Lett. **130B**(1983)171

3. M. Guttormsen, J. Rekstad, A. Henriquez, F. Ingebretsen and T.F. Thorsteinsen, Phys. Rev. Lett. **52**(1984)102

4. T. Ramsøy, J. Rekstad, M. Guttormsen, A. Henriquez, F. Ingebretsen, T.Rødland, T.F. Thorsteinsen and G. Løvhøiden, Nucl. Phys. **A438**(1985)301

5. M. Guttormsen, A. Ataç, F. Ingebretsen, T. Ramsøy, J. Rekstad, G. Løvhøiden, T. Rødland and T.F. Thorsteinsen, Selected Topics in Nuclear Structure, Proc. of XX Winter School Vol.1, Zakopane, Poland, 13-26 April 1985, p.81

6. S.M. Sie, J.O. Newton and R.M. Diamond, Nucl. Phys. **A367**(1981)176

7. A. Richter, Nucl. Spectr. and React. B, ed. J. Cerny, Academic Press (1974)343

8. Y.S. Chen and G. Leander, in Proceedings of the Conference of High Angular Momentum Properties of Nuclei, Oak Ridge, Tennessee, 1982 (Harwood, New York, 1982)

9. Y.S. Chen and G.A. Leander, Phys. Rev. **C26**(1982)2607

10. M.A. Preston, Physics of the Nucleus, Addison-Wesley Publishing Comp. Inc. (Massechusetts, 1963)

11. F. Puhlhofer,Nucl. Phys. **A280**(1977)267. The computer code CASCADE is modified by M.N. Harakeh, July 1983

Table 1: Properties of α-particle distributions

Target nucleus	Final nucleus	$< E_\alpha >$ (MeV)	FWHM (MeV)
^{162}Dy	^{161}Dy	53.0(5)	6.0(8)
	^{160}Dy	42.7(2)	11.9(20)
	^{159}Dy	31.4(2)	8.0(20)
	^{158}Dy	23.7(14)	10.0(20)
^{163}Dy	^{162}Dy	53.0(5)	6.8(6)
	^{161}Dy	45.5(7)	11.5(22)
	^{160}Dy	35.1(5)	11.5(20)
	^{159}Dy	26.6(9)	10.3(20)
	^{158}Dy	19.7(8)	6.8(6)

Figure caption:

Fig.1 The upper part shows the singles α-particle spectra. The lower part is obtained after subtraction of the contamination spectra.

Fig.2 Gamma-ray spectra from Ge detectors taken in coincidence with the α-particles.

Fig.3 Alpha-particle spectra produced with gates on γ-lines which belong to various Dy isotopes.

Fig.4 Decay level schemes for various Dy nuclei. For each nucleus the quoted intensities are normalized to the $4^+ - 2^+$ yrast transition.

Fig.5 Gamma-ray spectra of various Dy nuclei

Fig.6 The upper part shows the singles α-particle spectra. The coincidence α-particle spectra (middle part) are taken in coincidence with γ-rays from the NaI counters. The lower spectra show the γ-ray multiplicities as a function of α-particle energy.

Fig.7 The low excitation energy part of the multiplicity spectrum from the ^{163}Dy(^{3}He,α) reaction.

Fig.8 Average energy of evaporated neutrons from ^{162}Dy is shown as a function of excitation energy above the neutron threshold. The lack of experimental data between 5 and 7 MeV is due to impurities in the singles spectra (see fig.1).

Fig.9 Average energy of evaporated neutrons is shown as a function of the number of emitted neutrons. The squares show the results from the ^{162}Dy(^{3}He,α) reaction whereas the circles represent the results of the ^{163}Dy(^{3}He,α) reaction. The dashed curve is obtained from a statistical model calculation with the level density parameter $a = 13$ MeV^{-1}.

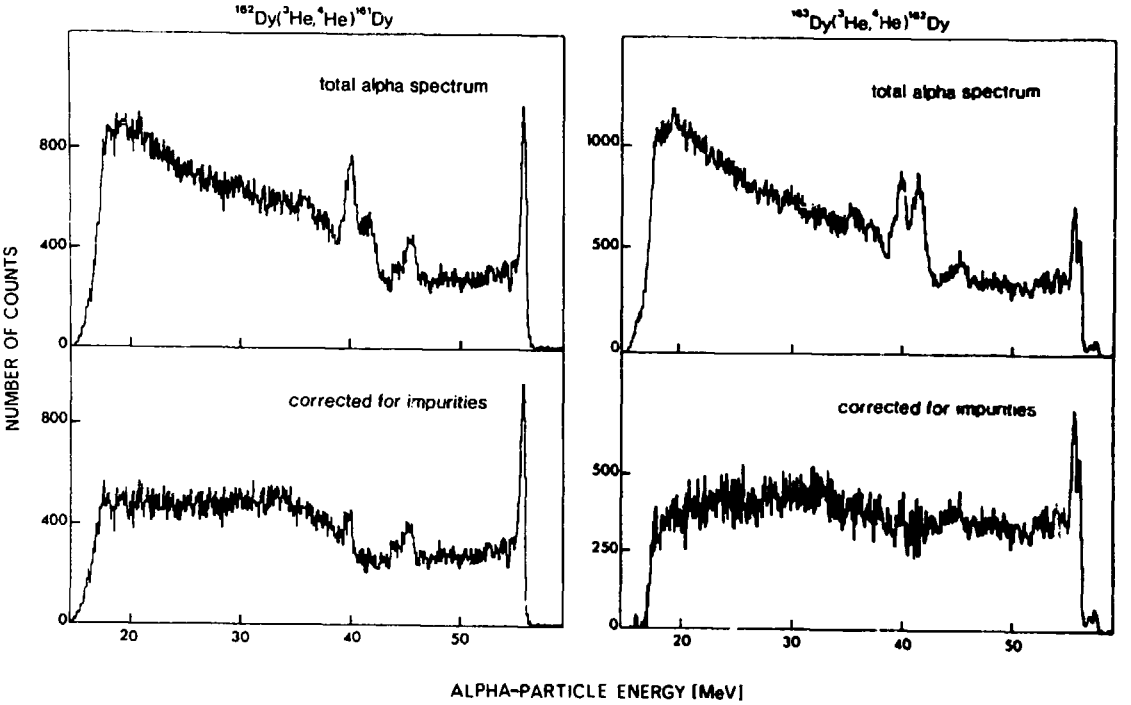
^{162}Dy(^{3}He,^{4}He)^{161}Dy
total alpha spectrum
corrected for impurities
^{163}Dy(^{3}He,^{4}He)^{163}Dy
total alpha spectrum
corrected for impurities
NUMBER OF COUNTS
ALPHA-PARTICLE ENERGY [MeV]

Fig.1

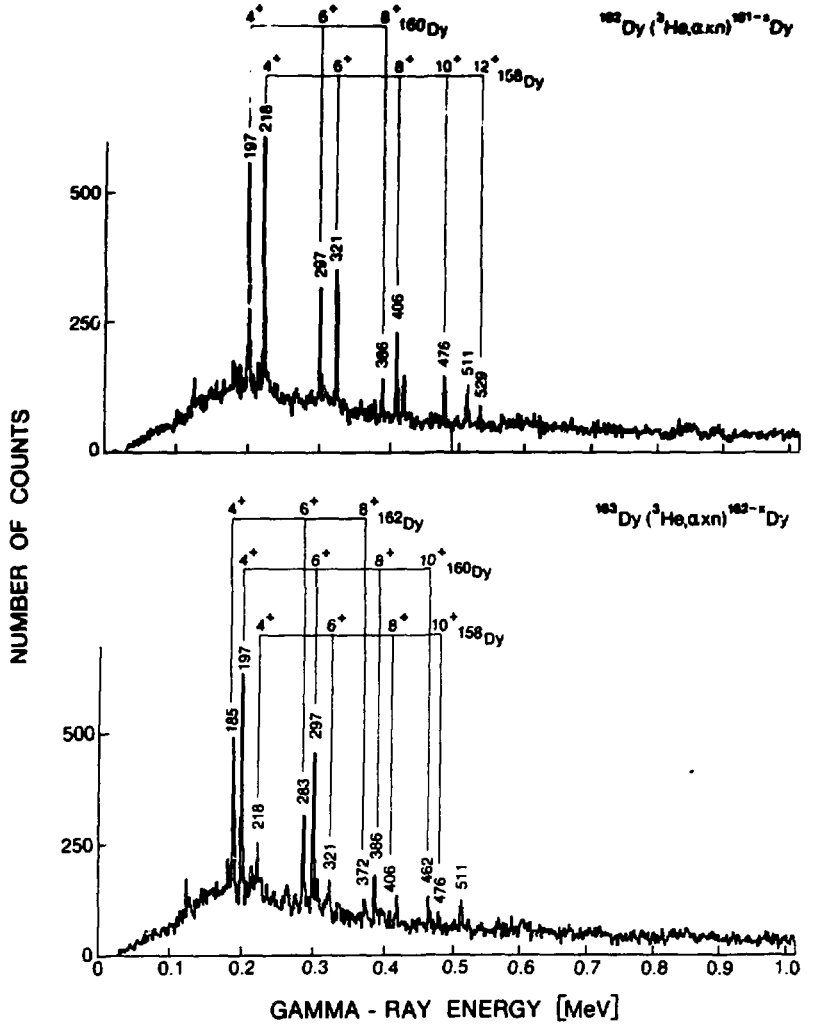
^{163}Dy (^{3}He,αxn)$^{161-x}$Dy
4+ 6+ 8+ 160Dy
4+ 6+ 8+ 10+ 12+ 158Dy
197
218
297
321
386
406
476
511
529
^{163}Dy (^{3}He,αxn)$^{162-x}$Dy
4+ 6+ 8+ 162Dy
4+ 6+ 8+ 10+ 160Dy
4+ 6+ 8+ 10+ 158Dy
185
197
218
263
297
321
372
386
406
462
476
511
NUMBER OF COUNTS
GAMMA - RAY ENERGY [MeV]

Fig.2

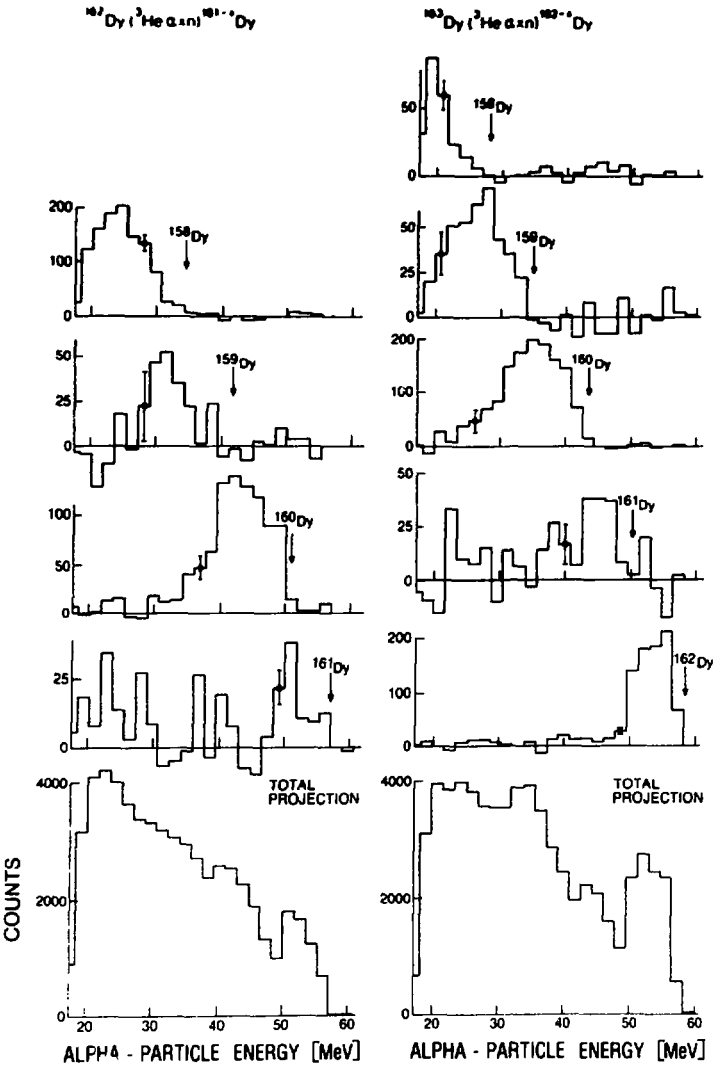
^{162}Dy (^{3}He α,xn)$^{161-x}$Dy
^{163}Dy (^{3}He α,xn)$^{162-x}$Dy
158Dy
159Dy
160Dy
161Dy
162Dy
TOTAL PROJECTION
COUNTS
ALPHA - PARTICLE ENERGY [MeV]

Fig.3

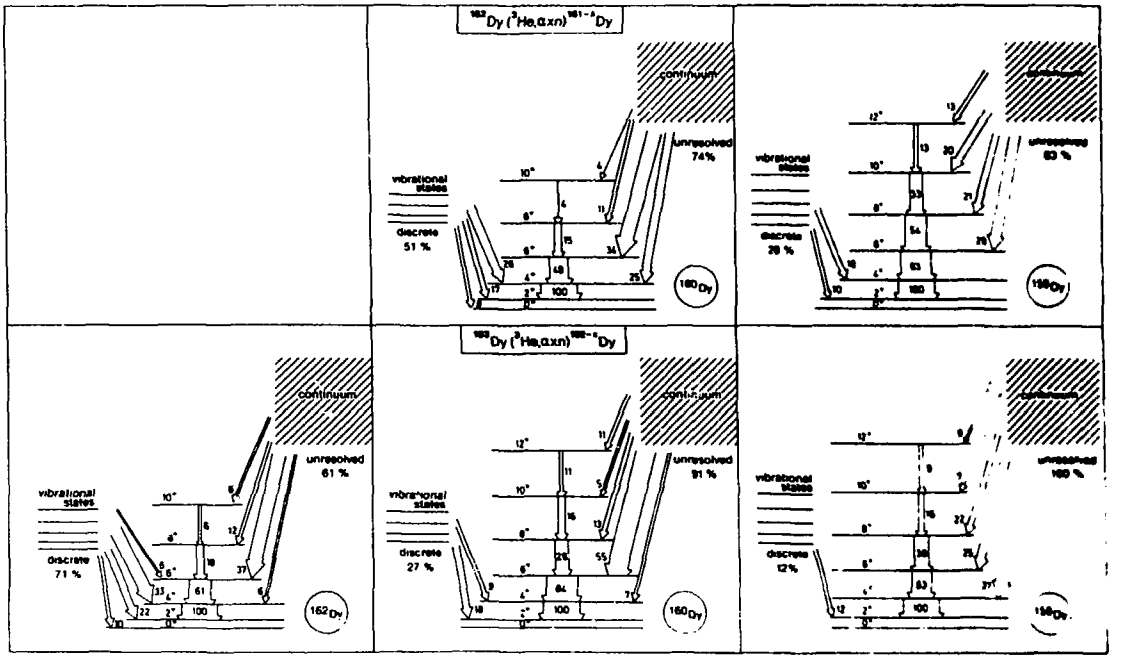
^{163}Dy (^{3}He,αxn)$^{161-x}$Dy
continuum
unresolved
74%
vibrational states
discrete
51 %
^{160}Dy
unresolved
63 %
discrete
29 %
^{158}Dy
^{162}Dy
unresolved
61 %
discrete
71 %
^{161}Dy (^{3}He,αxn)$^{160-x}$Dy
unresolved
91 %
discrete
27 %
^{160}Dy
unresolved
100 %
discrete
12 %
^{158}Dy

Fig.4

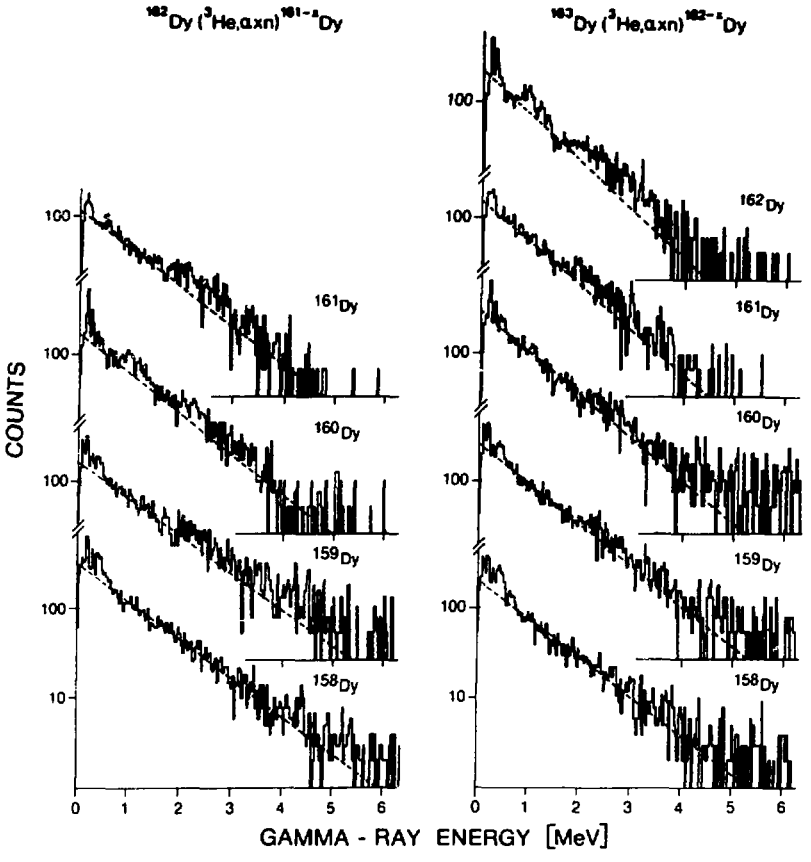
162Dy (3He,αxn)161-xDy
163Dy (3He,αxn)162-xDy
COUNTS
GAMMA - RAY ENERGY [MeV]
161Dy
160Dy
159Dy
158Dy
162Dy

Fig.5

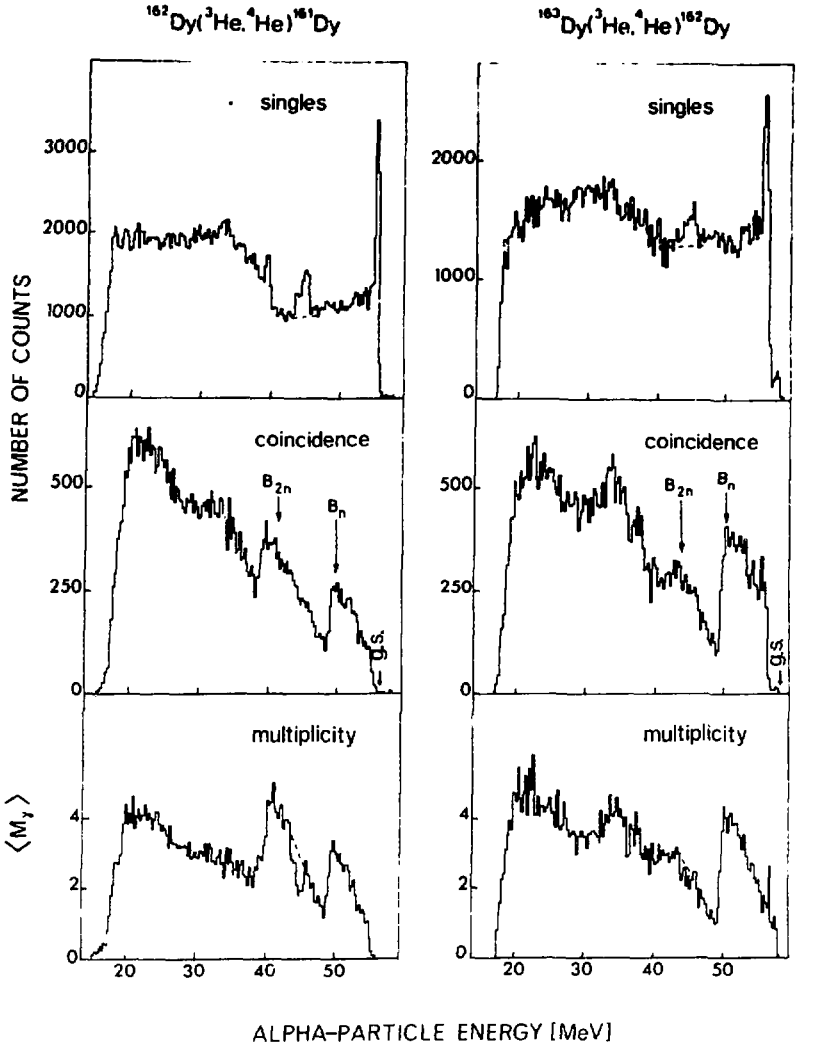
^{162}Dy(^{3}He,^{4}He)^{161}Dy
^{163}Dy(^{3}He,^{4}He)^{162}Dy
singles
coincidence
multiplicity
NUMBER OF COUNTS
$\langle M_\gamma \rangle$
B_{2n}
B_n
g.s.
ALPHA-PARTICLE ENERGY [MeV]

Fig.6

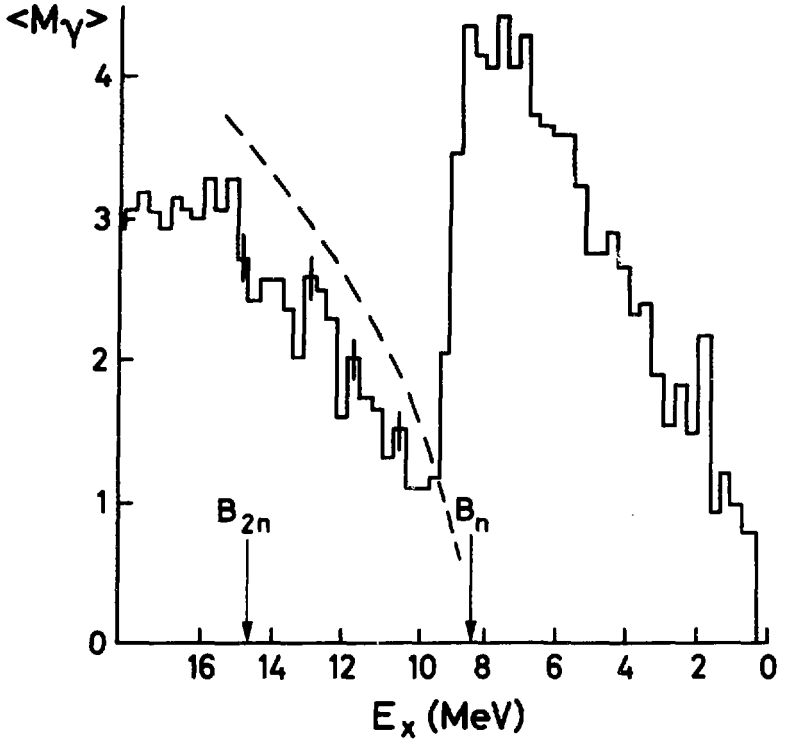

Fig.7

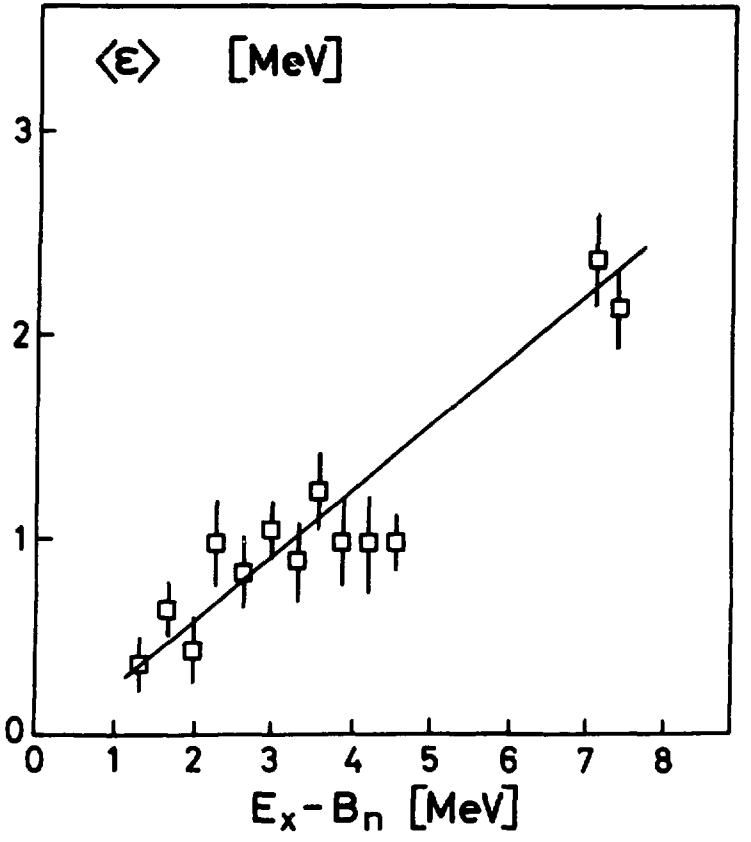

Fig.8

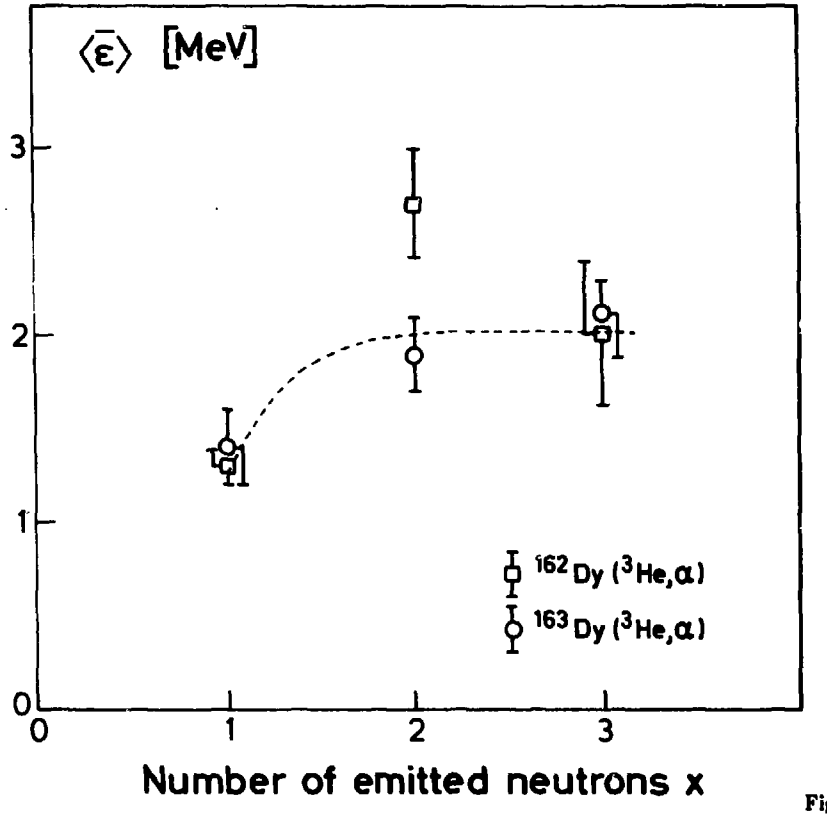
⟨ε̄⟩ [MeV]
3
2
1
0
0
1
2
3
162 Dy (3He,α)
163 Dy (3He,α)
Number of emitted neutrons x

Fig.9

FYSISK INSTITUTTS 8 FORSKNINGS-GRUPPER	DEPARTMENT OF PHYSICS RESEARCH SECTIONS
Allmennfysikk og didaktikk	General Physics
Biofysikk	Biophysics
Elektronikk	Electronics
Elementærpartikkel-fysikk	Experimental Elementary Particle physics
Faste stoffers fysikk	Condensed Matter physics
Kjernefysikk	Nuclear physics
Plasma-, molekylar- og kosmisk fysikk	Plasma-, Molecular and Cosmic physics
Teoretisk fysikk	Theoretical physics

ISSN - 0332 - 5571